Wireless Personal Communications (2020) 113:2519–2541
https://doi.org/10.1007/s11277-020-07339-6

Fractional S-Transform and Its Properties: A Comprehensive Survey

Rajeev Ranjan[1] · Neeru Jindal[2] · A. K. Singh[2]

Published online: 15 April 2020

Abstract

In time–frequency analysis, generalization of S-transform (ST) is known as fractional S-transform. Recently, fractional S-transform (FrST) has played an important role in the area of signal and image processing. The ST is a hybrid of wavelet, and short time Fourier transform. In this paper, the definition, properties and applications areas of ST and FrST are focused. The aim of this survey is to study ST and FrST, formats, properties, applications, and open issues to encourage further research in the fields of digital signal processing (DSP) and other applications area of engineering. In this article, firstly the several transforms that are related to ST as well as FrST are described and in the second part, comprehensive and exhaustive facts on the use of S-transform reviews and FrST in the area of DSP are enlightened. This transform technique is used for detection of LFM signal in the presence of echo.

Keywords S-transform (ST) · Wavelet transform (WT) · Short-time FT (STFT) · Fractional S-transform (FrST) · Fractional Fourier transform (FrFT)

1 Introduction

In the field of DSP the term 'Transform' is frequently used. The Transform is given this name because they transform one form of signal to another form of signal, so that it becomes easy to analyse or process than the original signal. Various types of transforms [1–7] and then different applications are demonstrated by different researchers like Fourier transform (FT) [8–15], fractional FT (FrFT) [16–21], short time FT (STFT) [22–25], Wavelet transform (WT) [26–33], fractional WT (FrWT) [27, 34, 35], S-transform (ST)

✉ Rajeev Ranjan
rajeevranjan1134@gmail.com

Neeru Jindal
neeru.jindal@thapar.edu

A. K. Singh
aaasma4u@gmail.com

1 Electronics & Communication Engineering Department, Chandigarh University, Gharuan (Mohali), Punjab, India

2 Thapar Institute of Engineering and Technology, Patiala, Punjab, India

[36–114] and fractional ST (FrST) [115–121]. In the FT technique, the analysed signal is either time or frequency. The time-domain signal exhibits information about the signal intensities and temporal evolution. For deterministic signals, analysis is usually based on instantaneous power spectrum or energy density spectrum. For random signals, the analysis tool depends on the auto-correlation functions and the power spectrum.

FT explores signal at various frequencies and their relative magnitudes. However, the main drawback of FT is that here no time resolution occurs, but frequency resolution occurs. That means FT can analyse the signal frequency response but cannot predict their location. To compensate this drawback, in the few decades several transforms techniques such as WT [122], Wigner transform [123], STFT [22, 23] and ST [38], and its fractional form came into existence. These techniques can represent a signal in time domain and frequency domain at the same time. However, WT cannot be used appropriately because infinite storage is required. Here no need to calculate dot-product between wavelet basis function and input signal. In WT only scale information can be expected with modulated phase information [38].

The drawback of Wigner transform is cross term, which is due to autocorrelation function. The cross terms produce noise or distortion in the signal analysis. The window size of fixed length is main drawback of STFT, hence it needs to be redefined. Therefore, STFT is not suitable for detecting the non-stationary signal where frequency is constantly changing according to instantaneous time. The STFT is usually not invertible in contrast of ST. Similarly, in the Gabor transform same problem occur due to fixed size Gaussian window. One case of non-stationary signal occur when the rotating machinery bearing breakdown in mechanical system then the defect signal received by the sensor is non-stationary in nature. Such signal contains time-bounded events. For the analysis of multicomponent and non-stationary signals, a time–frequency based method is traditional method based on either frequency or time domain. The time–frequency distributions give a 2-D representation that reflects the time-varying signals and shows the energy of distributed signal over 2-D time–frequency space. The ST gives a time–frequency representation in contrast with frequency representation by FT. At low frequency, multi resolution analysis is designed to obtain decent frequency and deficient resolution in time and vice versa at high frequency. ST and FrST is the most popular multi resolution tool that has been reviewed here. The concept behind the time–frequency joint representation is to distribute the signals into small parts followed by analysis of separate parts. In this way, the analysed signal gives more information about different frequencies [124–129].

The different time–frequency representation that exists in the literature is shown in Fig. 1. The first plot, in Fig. 1a, shows the way of representing the samples of a signal in time–frequency plane. It is clearly visible that the frequency information is absolutely lost in this method. Similarly, Fig. 1b shows the signal representation using Fourier transform.

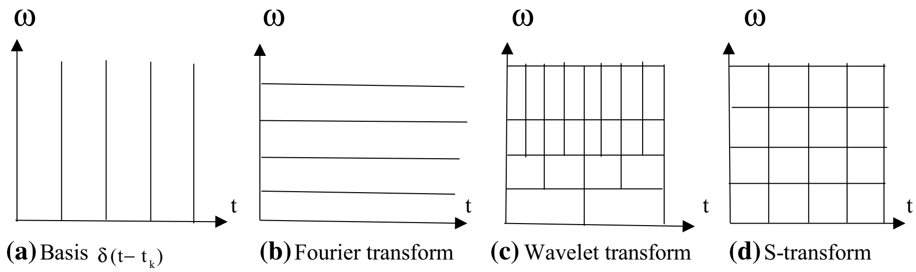

Fig. 1 Time–frequency representation method

In this method frequency axis is divided uniformly but the time axis information is entirely lost. Figure 1c depicts the time–frequency representation for wavelet transform. In this method, the scaling parameter of WT is inversely proportional to frequency. Therefore, the frequency resolution is decreasing for increasing frequency. S-transform representation is shown in Fig. 1d where the Gaussian window width is frequency dependent.

The width of the chosen window controls time–frequency representation in the transformed domain. ST mainly demonstrates some particular frequency segments in signal processing. It is a time–frequency restriction procedure with subordinate frequency resolution and compensates the drawback of STFT. To control the complex Fourier, signal ST is utilized as a window. However the window height and width are scaled by frequency. The response of ST shows frequency invariant amplitude in contrast with WT. It attenuates the high-frequency signals in contrast to low-frequency signals, and its generalized form is called FrST. The FrST improves FrFT and ST adaptability of signal analysis and generalized the time–frequency representation to time fractional frequency. Hence, FrST can upgrade the settling capacity and adaptability of signal analysis. Next section will demonstrate various transform with mathematical expressions.

2 Types of Transforms

Nowadays several transforms are used for various applications. Some of them are discussed in this section.

2.1 Fourier Transform (FT)

The FT is defined as a linear operator that maps a signal from time domain to an equivalent signal in frequency domain. It is also known as Fourier integral and mathematically defined as [1–4]

$$\mathrm{X(f)} = \int_{-\infty}^{\infty} \mathrm{x(t)} \exp(-\mathrm{j}2\pi \mathrm{ft})\, \mathrm{dt} \tag{1}$$

where X(f) is the FT of the signal x(t) and exp(−j2πft) is the basis function of FT. Similarly, the inverse-FT (IFT) is defined as [1–3]

$$\mathrm{x(t)} = \int_{-\infty}^{\infty} \mathrm{X(f)} \exp(\mathrm{j}2\pi \mathrm{ft})\mathrm{df} \tag{2}$$

The discrete FT (DFT) can be obtained by discretizing the both time and frequency axes into N samples and is defined [5–7] as

$$\mathrm{X[k]} = \sum_{\mathrm{n}=0}^{\mathrm{N}-1} \mathrm{x[n]} \exp\left(-\mathrm{j}\frac{2\pi \mathrm{kn}}{\mathrm{N}}\right); \quad \mathrm{k} = 0, 1, 2, \ldots, \mathrm{N}-1 \tag{3}$$

and inverse DFT (IDFT) is defined as [5, 6]

$$\mathrm{x[n]} = \frac{1}{\mathrm{N}} \sum_{\mathrm{k}=0}^{\mathrm{N}-1} \mathrm{X[k]} \exp\left(\mathrm{j}\frac{2\pi \mathrm{nk}}{\mathrm{N}}\right); \quad \mathrm{n} = 0, 1, 2, \ldots, \mathrm{N}-1 \tag{4}$$

2.2 Fractional Fourier Transform (FrFT)

The generalized form of FT with an angle α is called fractional FT (FrFT). It is defined for entire time–frequency plane where α is the counter clockwise angle from time-axis. Therefore, FrFT with $\alpha = \frac{\pi}{2}$ is FT. The FrFT with the angle α of a function $x(t)$ in transform-domain v in time–frequency plane is written as [16–20]

$$X(v) = \int_{-\infty}^{\infty} x(t)K_{\alpha}(t, v)dt \tag{5}$$

where

$$K_{\alpha}(t, v) = \begin{cases} B_{\alpha} \exp\left(j\pi(v^2 + t^2)\cot\alpha - j2\pi vt\csc\alpha\right); & \alpha \neq n\pi \\ \delta(t - v), & \alpha = 2n\pi \\ \delta(t + v), & \alpha = (2n - 1)\pi \end{cases} \tag{6}$$

and $B_{\alpha} = \sqrt{1 - j\cot\alpha}$, $n \in \mathbb{Z}$ and δ(t) is the unit impulse function. Here, $K_{\alpha}(t, v)$ is the basis function of FrFT. Similarly FrFT with respect to angle −α is called inverse fraction FT (IFrFT) and defined as [16, 17]

$$x(t) = \int_{-\infty}^{\infty} X(v)K_{\alpha}^{*}(t, v)dv \tag{7}$$

where ∗ represents the complex conjugate operation. The FrFT represents fractional spectrum; however, it has one major disadvantage of utilizing the global kernel. FrFT only provides spectral contents with no information around time confinement of FrFT spectrum parts. In this way, the exploration of a non-stationary signals that FrFT spectrum quality variation with time is still required.

2.3 Short Time-FT (STFT)

STFT is a classical transform for time–frequency analysis. In this transform, first the original signal x(t) multiplies with the window w(t − τ) and then computation of FT of the windowed signal is performed. FT change signal domain from time to frequency by coordinating over time axis. But for non-stationary signal, i.e., the frequency components are a function of time, at that point they can't point-out, when a specific frequency rises. The STFT overcome this drawback of FT by presenting a window w(t − τ). The window is intended to remove a little segment of continuous time signal x(t) and after that taking FT. The changed coefficient has two free parameters are frequency 'f' and time 'τ'. The STFT is written as [22–25]

$$X(\tau,\ f) = \int_{-\infty}^{\infty} x(t)w(t - \tau) \ldots \exp(-j2\pi ft)dt \tag{8}$$

and inverse STFT (ISTFT) is written as [22–25]

$$x(t) = \frac{1}{2\pi}\int_{-\infty}^{\infty}\int_{-\infty}^{\infty} X(\tau,\ f)w(t - \tau)\exp(j2\pi ft)d\tau df \tag{9}$$

2.4 Short-Time Fractional FT (STFrFT)

The short time FrFT (STFrFT) is improved form of FrFT for analysis of a non-stationary signal. The thought behind STFrFT was dividing the signals by utilizing a period over narrow window and acting the FrFT spectrum for every section. Since, the FrFT is calculated for every window section of the signal. STFrFT gives an accurate joint signal representation in both FrFT and time domain. It was introduced to improve their concentration and modify the STFT by using a window. The STFrFT was given in [18, 19], and versatile STFrFT is given in [20], here rotate a signal in time–frequency space by FrFT before executing STFT. A signal is multiplying with a window function called STFrFT. It is distinct as

$$\mathrm{STFrFT}(t, v) = \int_{-\infty}^{\infty} x(\tau)g(t-\tau)k(\tau, v)d\tau \tag{10}$$

In a few cases, the window function, with short time support is symmetry and real. However, fixed window width is a major disadvantage of STFrFT. Therefore, it did not give high resolution in FrFT and time domain. However, the efficacy of STFrFT is bounded using the uncertainty principle.

2.5 Wavelet Transform (WT)

Wavelet is used for the analysis of transient, time-varying or non-stationary phenomenon. It has energy concentrated in time and oscillating wave like characteristics. It can also allow instantaneous TF analysis with a mathematical definition. The main objective of WT is to define the basis function and to provide an efficient method for computations. In WT, a function x(t) is often be better defined or analyzed, if articulated as a linear decomposition using $x(t) = \sum_{l} a_l \varphi_l(t)$, where l represents integer index, $\varphi_l(t)$ is extension set and a_l is real-valued expansion coefficients. Similar to FT, WT defines with the extension of a set of basis function. Unlike to FT, WT does not expand in the trigonometric polynomial forms but expand in wavelet forms. The mother wavelet is observed that every application using fast FT (FFT) is formulated by wavelet to deliver more confined temporal and frequency information. In STFT, very small-frequency components cannot be detected in the spectral because fixed size window; however, WT overcomes this STFT problem. The wavelet analysis is considered as a complex function that satisfy the following circumstances [27–33]

$$\int_{-\infty}^{\infty} |\psi(t)|^2 < \infty \tag{11}$$

$$C_\psi = 2\pi \int_{-\infty}^{\infty} \frac{|\Psi(\omega)|^2}{|\omega|} d\omega < \infty \tag{12}$$

where Ψ is FT of mother wavelet function ψ. Here, condition (11) gives finite energy of wavelet function ψ and (12) is admissibility condition, indicates that if $\Psi(\omega)$ it is smooth, then $\Psi(\omega) = 0$.

2.5.1 Continuous Wavelet Transform (CWT)

If wavelet function ψ fulfils the above conditions, then WT of a function x(t) and wavelet function ψ(t) is written as [121, 130]

$$X(b,a) = \frac{1}{\sqrt{a}} \int_{-\infty}^{\infty} x(t)\psi^{*}\left(\frac{t-b}{a}\right) dt \tag{13}$$

$$X(b,a) = \int_{-\infty}^{\infty} x(t)\psi_{a,b}^{*} dt \tag{14}$$

where $\psi_{a,b} = \frac{1}{\sqrt{a}}\psi\left(\frac{t-b}{a}\right)$ and ψ^{*} represent the complex conjugate of wavelet function ψ and defined on open interval (b, a) half plane ($b \in \mathbb{R}, \quad a > 0$), where the scale of analysing and time shifting wavelet represented by a and b respectively. The signal x(t) is achieved from WT and X(b, a) by the inversion formula. The inverse CWT (ICWT) is written as

$$x(t) = \frac{1}{C_{\psi}} \int_{-\infty}^{\infty} \int_{-\infty}^{\infty} \frac{X(b,a)\,\psi_{a,b}(t)}{a^{2}}\, da\, db \tag{15}$$

2.5.2 Discrete Wavelet Transform (DWT)

In discrete form of WT, scale and shift factors are discretized as $a = a_0^m$ and $b = nb_0$. Therefore, wavelet is also discretized as

$$\psi_{m,n}(t) = a_0^{-\frac{m}{2}}\, \psi\left(\frac{t - nb_0}{a_0^m}\right) \tag{16}$$

where m and n are an integers. The DWT is defined as [27, 28]

$$X_{m,n} = \int_{-\infty}^{\infty} x(t)\, \psi_{m,n}^{*}(t) dt \tag{17}$$

and inverse DWT (IDWT) is defined in [27, 28] as

$$x(t) = k_{\psi} \sum_{m} \sum_{n} X_{m,n} \psi_{m,n}(t) \tag{18}$$

where normalization constant is k_{ψ}. In the scale time plane function $\psi_{m,n}(t)$ gives the sampling points, linear sampling in time direction but logarithmic in scale direction. In general, a_0 is chosen as $a_0 = 2^{\frac{1}{J}}$, where, J is an integer value [27]. The generalized form of wavelet called fractional WT is given in the next part.

2.6 Fractional Wavelet Transform (FrWT)

Fractional WT (FrWT) is a generalized form of WT with an angle parameter α, but when the angle α is $\frac{\pi}{2}$, FrWT is similar to WT. FrWT rectifies the limitation of WT and FrFT. FrWT with an angle α of a continuous function x(t) defined as [27, 34, 35]

$$W_x^{\alpha}(a,b) = \int_{\mathbb{R}} x(t)\varphi^*_{\alpha,a,b}(t)dt \tag{19}$$

and transform kernel defined as [27, 34, 35]

$$\varphi_{\alpha,a,b}(t) = \frac{1}{\sqrt{a}}\varphi\left(\frac{t-b}{a}\right)\exp\left(-j\frac{t^2-b^2}{2}\cot\alpha\right) \tag{20}$$

where $a \in \mathbb{R}^+$,$b \in \mathbb{R}$ and $x(t) \in L^2(\mathbb{R})$. Similar to FrFT, FrWT gets compensations of multiresolution analysis (MRA) of WT, which has fractional domain signal representation capability.

2.7 S-Transform (ST)

S-transform (ST) is hybrid of WT and STFT in time–frequency domain. It overcomes the drawbacks of STFT and deficiency of phase in WT. ST utilizes a Gaussian function, that width and height is constrained by frequency. The ST gives signal clarity in contrast to different transforms since it doesn't have cross terms issues. ST displays invariant frequency amplitude in compare with WT and also analysed phase and power spectrums. The ST diminishes high-frequency as compare to low-frequency signal [2, 3]. ST of a signal 'x(t)' is represented by $X(\tau, f)$ and defined as [1–3]

$$X(\tau,\ f) = \int_{-\infty}^{\infty} x(t)g(t-\tau, f)\exp(-j2\pi f t)\,dt \tag{21}$$

$$X(\tau,\ f) = \int_{-\infty}^{\infty} x(t)\frac{|f|}{\sqrt{2\pi}}\exp\left(\frac{-(t-\tau)^2 f^2}{2}\right)\exp(-j2\pi ft)\,dt \tag{22}$$

where Gaussian function, $g(t-\tau,\ f)$ controlled by frequency 'f' and time shift 'τ'. If $X(\tau,\ f)$ is integrated with respect to 'τ' then, it give FT of x(t), written as

$$\int_{-\infty}^{\infty} X(\tau,\ f)\,d\tau = \int_{-\infty}^{\infty}\left(\int_{-\infty}^{\infty} x(t).g(t-\tau,\ f)\exp(-j2\pi ft)dt\right)d\tau \tag{23}$$

Using the normalized condition of the Gaussian function is written as

$$\int_{-\infty}^{\infty} g(t-\tau,\ f)d\tau = \int_{-\infty}^{\infty}\frac{|f|}{\sqrt{2\pi}}\exp\left(\frac{-(t-\tau)^2 f^2}{2}\right)d\tau = 1 \tag{24}$$

and (23) can be written as

$$\int_{-\infty}^{\infty} X(\tau,\ f)\, d\tau = \int_{-\infty}^{\infty} x(t)\ \exp(-j2\pi ft)\, dt = X(f) \tag{25}$$

where FT of x(t) is represented by X(f).

The two-dimensional ST (2-D ST) is written as

$$X(\tau_1,\tau_2,f_1,f_2) = \int_{-\infty}^{\infty}\int_{-\infty}^{\infty} x(t_1,t_2)\frac{|f_1||f_2|}{2\pi}\exp\left(-\frac{(t_1-\tau_1)^2 f_1^2}{2} - \frac{(t_2-\tau_2)^2 f_2^2}{2}\right)\exp(-j2\pi(f_1 x + f_2 y))\,dt_1 dt_2 \tag{26}$$

The two-dimensional inverse S-transform (2-DIST) is defined as

$$x(t_1,t_2) = \int_{-\infty}^{\infty}\int_{-\infty}^{\infty}\left(\int_{f_{1l}}^{f_{1h}}\int_{f_{2l}}^{f_{2h}} X(\tau_1,\tau_2,f_1,f_2)d\tau_1 d\tau_2\right)\exp(j2\pi(f_1 x + f_2 y))\,df_1 df_2 \tag{27}$$

2.7.1 Discrete S-Transform (DST)

Due to the advent of discrete systems, the discretization of every mathematical tool becomes necessary to increase the span of its applications. Considering the discrete version of the signal x(t) as x[kT] where, k = 0,1,2, … , N − 1 and sampling interval T, its discrete FT (DFT) is given by [1]

$$X\left[\frac{n}{NT}\right] = \frac{1}{N}\sum_{k=0}^{N-1} x[kT]\ \exp\left(-\frac{j2\pi nk}{N}\right) \tag{28}$$

where,n = 0,1,2, … , N − 1. For discrete, ST is the projection of vectors define using time sequences x[kT] over vector a set of vectors. Using (22), in Discrete case of x[kT] can be defined [1–4] as

$$X\left[iT,\frac{n}{NT}\right] = \sum_{m=0}^{N-1} x\left[\frac{m+n}{NT}\right]\ \exp\left(-\frac{2\pi^2 m^2}{n^2}\right)\exp\left(\frac{j2\pi mi}{N}\right);\quad n \neq 0 \tag{29}$$

For n = 0, it is written as

$$X[iT]=\frac{1}{N}\sum_{m=0}^{N-1} x\left[\frac{m}{NT}\right] \tag{30}$$

where,i, m and n = 0, 1, 2, … , N − 1. The inverse discrete ST (IDST) is defined as [1, 2]

$$x[kT]=\sum_{n=0}^{N-1}\left(\frac{1}{N}\sum_{i=0}^{N-1} X\left[iT,\frac{n}{NT}\right]\right)\exp\left(\frac{j2\pi nk}{N}\right) \tag{31}$$

Subsequently, in literature, other definitions of discrete S-transform were also reported [9]. Here one such definition is presented, which was called as Discrete Orthonormal ST (DOST) [9–11], which is defined in terms of 'N' unit length basis vector, which as:

$$X[kT]_{[v,\beta,\tau]} = \frac{1}{\sqrt{\beta}} \sum_{f=v-\beta/2}^{v+\beta/2+1} \exp\left(j2\pi\frac{\tau}{\beta}f\right).\exp\left(-j2\pi\frac{k}{N}f\right).\exp(-j2\pi\tau); \quad k = 0,1,2,\dots,N-1 \tag{32}$$

$$X[kT]_{[v,\beta,\tau]} = \frac{\exp\left(-j2\alpha\left(\frac{2v-\beta-1}{2}\right)\right) - \exp\left(-j2\alpha\left(\frac{2v+\beta-1}{2}\right)\right)}{2\sqrt{\beta}\sin\alpha} j\exp(-j2\pi\tau) \tag{33}$$

where $\alpha = \pi\left(\frac{k}{N} - \frac{\tau}{\beta}\right)$ is a center of the temporal window for kth basis vector. Mathematically, these basis vectors are orthonormal

$$\frac{1}{N}\int_0^N X[kT]_{[\nu',\beta',\tau']} X^*[kT]_{[v,\beta,\tau]} dk = \delta_{\nu' v}\delta_{\beta'\beta}\delta_{\tau'\tau} \tag{34}$$

where $\delta_{\nu' v} = \begin{cases} 1; & \nu' = v \\ 0; & \text{else} \end{cases}$ is a delta function. The discrete inverse ST (IDST) is defined as

$$x[kT] = \sum_{n=0}^{N-1}\left(\frac{1}{N}\sum_{i=0}^{N-1} X\left[iT, \frac{n}{NT}\right]\right)\exp\left(\frac{j2\pi nk}{N}\right) \tag{35}$$

In Table 1 described the basis function of different transforms.

2.7.2 Relation Between ST and Others Types of Transforms

The relation between ST and some other types of transform is given as

(i) Relation between ST and STFT

STFT of a function x(t) is defined in (8), and the ST is defined in (22). ST is considered as a specific type of STFT with a Gaussian window function.

The STFT of a signal x(t) is defined as [6]

$$STFT(\tau, f) = \int_{-\infty}^{\infty} x(t)\, w(t-\tau)\exp(-j2\pi f\, t)\, dt \tag{36}$$

where, $w(t-\tau)$ is represent window function.

Table 1 Basis of the transforms

Transforms	Basic functions
FT	The complex exponential function with different frequency that is $\exp(j2\pi ft)$
STFT	The windowed or truncated complex exponential function that is $w(t-\tau)\exp(j\xi t)$
WT	Translated and scaled form of mother wavelet that is $\frac{1}{\sqrt{a}}\psi\left(\frac{t-b}{a}\right)$
ST	The Gaussian windowed complex exponential function that is, $\frac{\lvert f\rvert}{\sqrt{2\pi}}\exp\left(\frac{-(t-\zeta)^2 f^2}{2}\right)\exp(-j2\pi ft)$

Table 2 Existing properties of S-transform

Properties	Mathematical equations
Linearity	$\{a\,x(t) + by(t)\} \overset{ST}{\Leftrightarrow} a\,X(\tau,\ f) + b\,Y(\tau,\ f)$
Scaling	$x(kt) \overset{ST}{\Leftrightarrow} \frac{1}{\lvert k\rvert} X\left(k\tau,\ \frac{f}{k}\right)$
Time shifting	$X\left(t - \tau_0\right) \overset{ST}{\Leftrightarrow} \exp(-j2\pi f\tau_0) X\left(\tau - \tau_0,\ f\right)$
Time reversal	If $y(t) \overset{ST}{\Leftrightarrow} Y(\tau,\ f)$; then $y(-t) \overset{ST}{\Leftrightarrow} Y^*(-\tau,\ f)$
Time derivatives	If, $y(t) \overset{ST}{\Leftrightarrow} Y(\tau,\ f)$ then, $\frac{d\{y(t)\}}{dt} \overset{ST}{\Leftrightarrow} j(2\pi f).Y(\tau,\ f)$
Complex conjugate	If $y(t) \overset{ST}{\Leftrightarrow} Y(\tau,\ f)$ then, $y^*(t) \overset{ST}{\Leftrightarrow} Y^*(\tau, -f)$
Cross-correlation	The function x(t) and y(t) is denoted by z(t) then the weighted correlation is defined as $z(t) = \int_{-\infty}^{\infty} y(t+\xi)\, x^*(\xi) \exp\left(-\left(\xi - {}^{\tau}/_{2}\right)\left(t + \xi - {}^{\tau}/_{2}\right) f^2\right) d\xi$ then, cross-correlation of ST is defined as [39] $z(t) = \int_{-\infty}^{\infty} y(t+\xi) x^*(\xi) \exp\left(-\left(\xi - {}^{\tau}/_{2}\right)\left(t + \xi - {}^{\tau}/_{2}\right) f^2\right) d\xi \overset{ST}{\Leftrightarrow} \frac{\sqrt{2\pi}}{\lvert f\rvert} X^*\left({}^{\tau}/_{2}, f\right) Y\left({}^{\tau}/_{2}, f\right) = Z(\tau,\ f)$ where, '$*$' represent the complex conjugate
Convolution theorem	The function p(t) and q(t) is denoted by r(t) then, the weighted convolution is define as $r(t) = \int_{-\infty}^{\infty} q(t-\xi) p(\xi) \exp\left(\left(t - \xi - {}^{\tau}/_{2}\right)\left(\xi - {}^{\tau}/_{2}\right) f^2\right)\, d\xi$ then, convolution of ST is defined as [39] $r(t) = \int_{-\infty}^{\infty} q(t-\xi) p(\xi) \exp\left(\left(t - \xi - {}^{\tau}/_{2}\right)\left(\xi - {}^{\tau}/_{2}\right) f^2\right) d\xi \overset{ST}{\Leftrightarrow} \frac{\sqrt{2\pi}}{\lvert f\rvert} P\left({}^{\tau}/_{2},\ f\right)\, Q\left({}^{\tau}/_{2},\ f\right) = R(\tau,\ f)$
Parseval's theorem	The Parseval's theorem of ST is defined as [39]

$$X(\tau, f) = \int_{-\infty}^{\infty} x(t)\, g(t-\tau, f)\, \exp(-j2\pi f t)dt \tag{37}$$

where Gaussian function, $g(t-\tau, f)$ controlled by frequency 'f' and time shift 'τ'. Hence, after the comparative analysis, concluded that ST is a specific instance of the STFT with a Gaussian window function.

(ii) Relation between ST and CWT

The WT of a signal x(t) defined as [8]

$$W(\tau, d) = \int_{-\infty}^{\infty} x(t)\, m(t-\tau, d)dt \tag{38}$$

where τ and d represents, the time of spectral localization and dilation factor respectively. The dilation factor decides the 'width' of the wavelet and thus, it controls the resolution. W(τ, d) denoted by a scaled copy of the fundamental mother wavelet and must have zero mean [2]. Hence, after the comparative analysis, the ST is derived, when WT multiplied by the phase factor, thus the ST can be defined as

$$X(\tau, f) = W(\tau, d)\, \exp(-j2\pi f\tau) \tag{39}$$

where the mother wavelet is defined as

$$m(t,f) = \frac{|f|}{\sqrt{2\pi}} \exp\left(\frac{-t^2 f^2}{2}\right) \exp(-j2\pi f t) \tag{40}$$

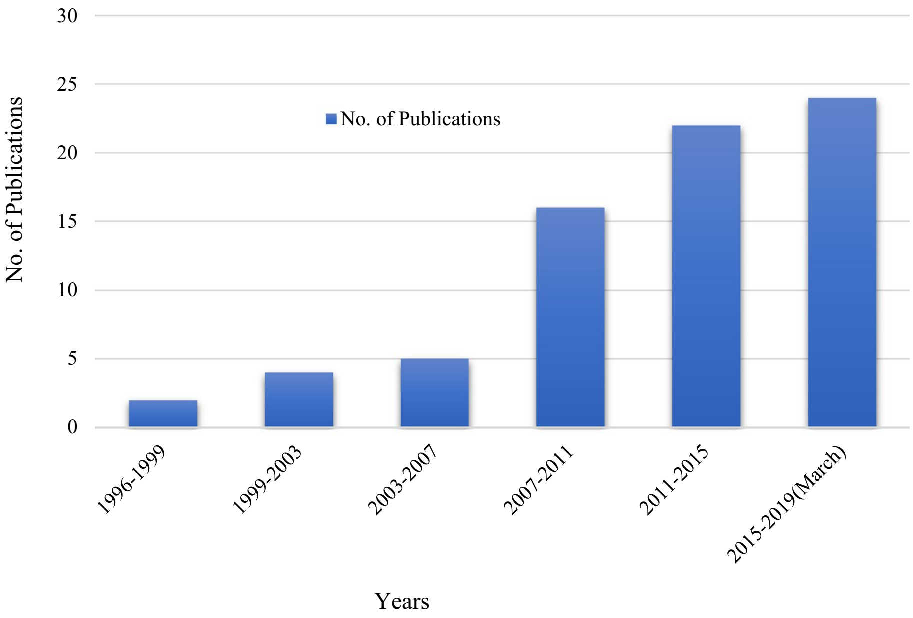

Fig. 2 Number of publications in S-transform

Table 3 Applications of S-transform

Applications	References
Geo-informatics	Stockwell et al. [36], Adams et al. [37], Aldas et al. [40], Hindley et al. [45], Huang et al. [46], Gao et al. [47], Ghaffarzadeh et al. [48], Hutnikova et al. [57], Ditommaso et al. [58], Battisti et al. [59], Zhao et al. [60], Ma et al. [109]
Image processing	Mansinha et al. [49], Sahoo et al. [67], Drabycz et al. [68], Jiang et al. [69], Badrinath et al. [70], Zhong et al. [71, 72], Shen et al. [73], Dash et al. [74], Saedi et al. [75], Kumar et al. [76, 78], Nithya et al. [77], Wang et al. [79–82]
Signal processing	Ranjan et al. [39, 107], Sejdic et al. [41], Guo et al. [42], Lin et al. [43], Pinneger et al. [50], Schimmel et al. [51], Stockwell et al. [52], Pie et al. [53], Assous et al. [54], Singh et al. [55, 56], Battisti et al. [59], Hamidia et al. [61], Yin et al. [62], Weishi et al. [65], Zidelmal et al. [66]
Bio-medical signal processing	Das et al. [83], Ari et al. [84], Agrawal et al. [85], Zidelmal et al. [86], Harisaran et al. [87], Yusof et al. [88], Ortiz et al. [92], Perez et al. [93], Roy et al. [98]
Power system	Xiao et al. [94], Behera et al. [95], Li et al. [96], Uyar et al. [97], Borin et al. [100], Zhang et al. [105], Mahela et al. [106]
Communication	Roy et al. [98]

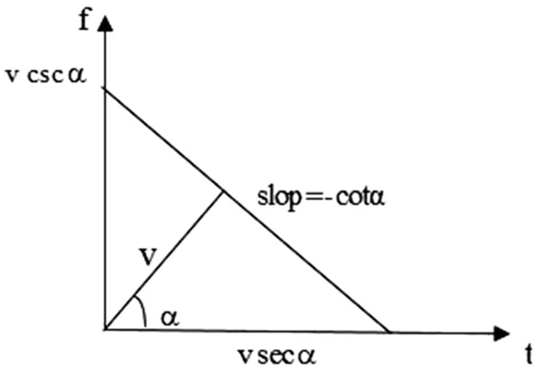

Fig. 3 The time-fractional frequency plane

where the dilation factor ‘d’is inverse of the frequency ‘f’. The ST gives better, dependent frequency resolution in time frequency analysis with least noise.

(iii) Relation between FT and ST

The above definition of FT and ST of function x(t) give a relation between FT and ST is written as

$$X(f) = \int_{-\infty}^{\infty} X(\tau,\ f)\, d\tau \tag{41}$$

Hence, using FT, inverse ST (IST) is defined as [36]

$$x(t) = \int_{-\infty}^{\infty} \left\{ \int_{-\infty}^{\infty} X(\tau,\ f)\, d\tau \right\} \exp(j2\pi ft)\, df \tag{42}$$

Table 4 Existing properties of fractional ST

Properties	Mathematical formulation
Linearity property	If, $z(t) = a\,x(t) + b\,y(t)$ then, $Z^{\alpha}(\tau, v) = a\,X^{\alpha}(\tau, v) + b\,Y^{\alpha}(\tau, v)$ where, a and b are constant
Scaling property	$X^{\alpha}_{x(ct)}(\tau, v)=\sqrt{\frac{c^2(1-j\cot\alpha)}{c^2-j\cot\alpha}}\exp\left(j\pi v^2\cot\alpha\left(1-\frac{\cos^2\beta}{\cos^2\alpha}\right)\right) X^{\alpha}\left(c\tau, v\frac{\sin\beta}{\cos^2\alpha}\right)$ where, $b=\frac{2\beta}{\pi}$ and $\beta=\tan^{-1}\left(c^2\tan\alpha\right)$
Time reversal	$Y^{\alpha}_{y(-t)}(\tau, v) = Y^{\alpha}(-\tau, -v)$
Time-marginal condition	$\int_{-\infty}^{\infty} Y^{\alpha}(\tau, v)d\tau = \int_{-\infty}^{\infty} y(t)\kappa_{\alpha}(t, v)\,dt = Y^{\alpha}(v)$ where $X^{\alpha}(v)$ is FT of x(t)
Inverse fractional S-transform	$y(t) = \int_{-\infty}^{\infty}\left(\int_{-\infty}^{\infty} Y^{\alpha}(\tau, v)d\tau\right)\kappa^{*}_{\alpha}(t, v)dv$
Cross-correlation theorem	The weighted cross-correlation is defined as $r(t) = B_{\alpha}\int_{-\infty}^{\infty} q(t+\xi)\,p^{*}(\xi)\ \exp\left(-\left\{\tau t - 2\tau\xi + 2\xi(t-\xi) - {}^{\tau^2}\!/_2\right\}{}^{(v\csc\alpha)^2}\!/_2 + j\pi\left\{v^2 + 2\xi(t+\xi)\right\}\cot\alpha\right)d\xi$ Then, cross-correlation of FrST is written in [130] as $r(t) = B_{\alpha}\int_{-\infty}^{\infty} q(t+\xi)p^{*}(\xi)\ \exp\left(-\left\{\tau t - 2\tau\xi + 2\xi(t-\xi) - {}^{\tau^2}\!/_2\right\}{}^{(v\csc\alpha)^2}\!/_2 + j\pi\left\{v^2+2\xi(t+\xi)\right\}\cot\alpha\right)d\xi$ $\overset{S^{\alpha}}{\Leftrightarrow} \frac{\sqrt{2\pi}}{\lvert v\csc\alpha\rvert}P^{\cdot}\left({}^{\tau}\!/_2, v\right) Q^{\cdot}\left({}^{\tau}\!/_2, v\right)$ where, $*$ represent complex conjugate and $B_{\alpha}=\sqrt{1-j\cot\alpha}$
Convolution theorem	The weighted convolution is defined as $Z(t) = B_{\alpha}\int_{-\infty}^{\infty} x(t-\xi)\,y(\xi)\ \exp\left(-\left\{\tau(t-\tau) - 2\xi(t-\xi)+\tau\xi - {}^{\tau^2}\!/_2\right\}{}^{(v\csc\alpha)^2}\!/_2 + j\pi\left\{v^2 - 2\xi(t-\xi)\right\}\cot\alpha\right)d\xi$ Then, convolution of FrST is written in [130] as $z(t) = B_{\alpha}\int_{-\infty}^{\infty} x(t-\xi)\,y(\xi)\ \exp\left(-\left\{\tau\xi - 2\xi(t-\xi) + \tau(t-\tau) - {}^{\tau^2}\!/_2\right\}\frac{(v\csc\alpha)^2}{2} + j\pi\left\{v^2 - 2\xi(t-\xi)\right\}\cot\alpha\right)d\xi$ $\overset{S^{\alpha}}{\Leftrightarrow} \frac{\sqrt{2\pi}}{\lvert v\csc\alpha\rvert}X^{\alpha}\left({}^{\tau}\!/_2, v\right)Y^{\alpha}\left({}^{\tau}\!/_2, v\right)$ where, FRST is denoted by S^{α}
Parseval's theorem	The Parseval's theorem of FrST is defined as [130]

2.7.3 Properties of S-Transform

Based on the survey [39], there are many existing properties of ST as defined in Table 2.

Figure 2 shows that the application of ST is increases yearly, where the maximum publications are in the year of 2015 to 2019.

Table 3 described the different applications of ST in different area of Geo-informatics, Image processing, Signal processing, Bio-medical, Power system and Communication by several authors.

2.8 Fractional S-Transform (FrST)

The FrST was first introduced in 2012 [115], as a way to deal with synthetic Ricker wavelet and seismic data. It is defined as a cascade of FrST and ST. The Fig. 3 show, time-fractional frequency plane in FrST domain.

In 2012, [115] expressed ST of a signal in terms of FrFT and Gaussian window, they are also known as FrST. Actually authors originate an equivalent expression of ST in FrFT domain. FrST of a function x(t) with an angle α is written in [115–117] as

$$X^{\alpha}(\tau, \mathrm{v}) = \int_{-\infty}^{\infty} \mathrm{x(t)g}(\tau - \mathrm{t, v})\kappa_{\alpha}(\mathrm{t, v})\mathrm{dt} \tag{43}$$

where ‘v’ is fractional frequency. The FrST is function of fractional frequency (v) and time (t) and Gaussian function $g(\tau - t, v)$ is scalable with ‘t’ and FrFT frequency ‘v’.

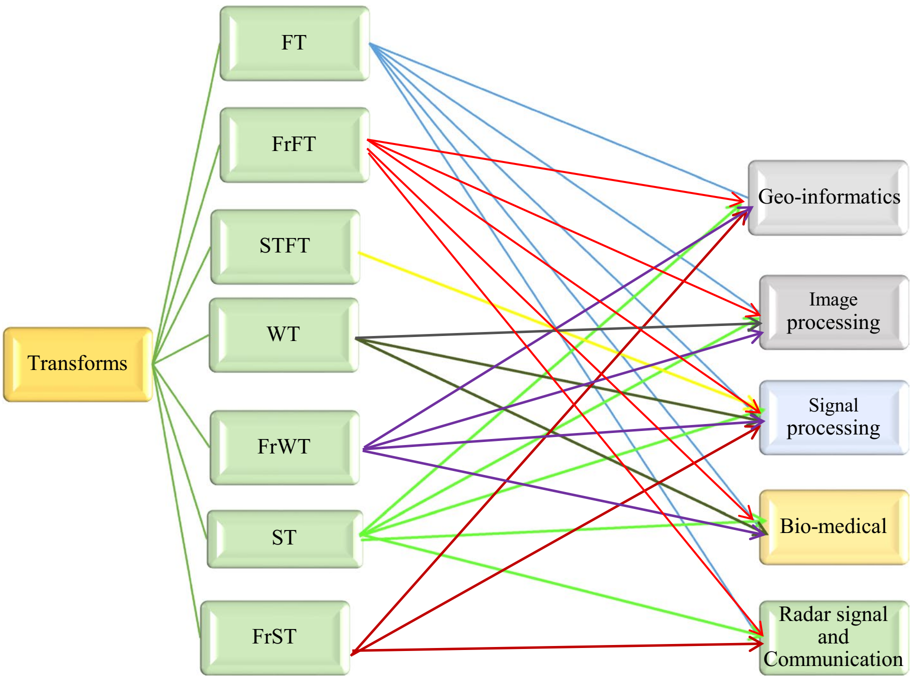

Fig. 4 Applications of transforms

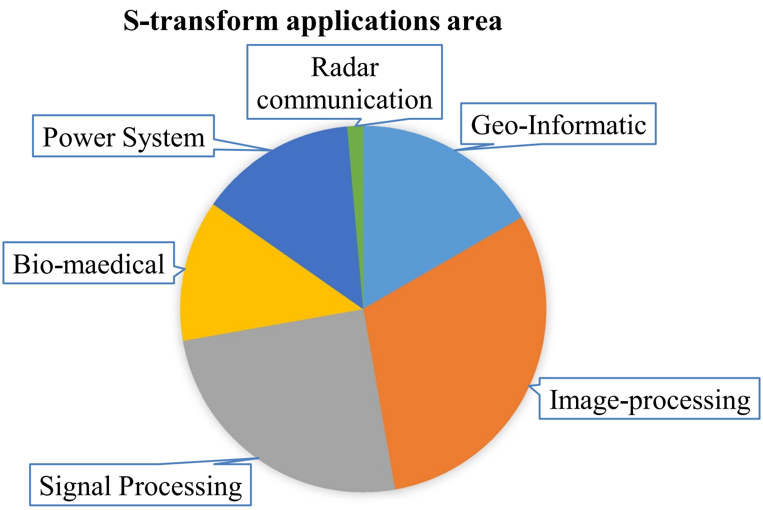

Fig. 5 Graphical presentation of S-transform application

$$g(t,\ v)=\frac{|v(\csc\alpha)|^{p}}{\sqrt{2\pi}q}\exp\left(\frac{-t^{2}\{v(\csc\alpha)\}^{2p}}{2q^{2}}\right) \tag{44}$$

where transformation kernel $\kappa_\alpha(t, v)$ is defined in (2) and $\alpha=\frac{a\pi}{2}$. In (7) the Gaussian function varies with frequency. The fractional factor $a \in [0, 4]$ and rotation angle $\alpha=\frac{a\pi}{2}$, with $p = q = 1$ and $a = 1$, then FrST coincides with ST as

$$X(\tau,\ v) = \int_{-\infty}^{\infty} x(t)\frac{|v|}{\sqrt{2\pi}}\ \exp\left(-\frac{(t-\tau)^2 v^2}{2}\right)\exp(-j2\pi vt) \tag{45}$$

The generalized form of ST is called FrST, it is better than ST and FrFT. The FrST is improve the flexibility of time–frequency analysis and energy of signal spectra. FrST can efficiently improve the time–frequency resolution capacity as compared to ST.

The inverse FrST (IFrST) is given as [115]

$$x(t) = \int_{-\infty}^{\infty}\left\{\int_{-\infty}^{\infty} X^*(\tau, v)d\tau\right\}\kappa_\alpha^*(t, v)dv \tag{46}$$

where '*' represents complex conjugate.

According to [115] marginal condition of FrST yield,

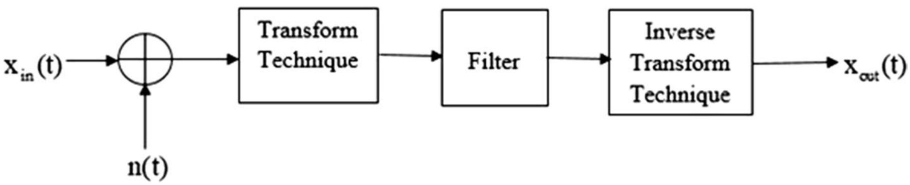

Fig. 6 Filtering of LFM signal

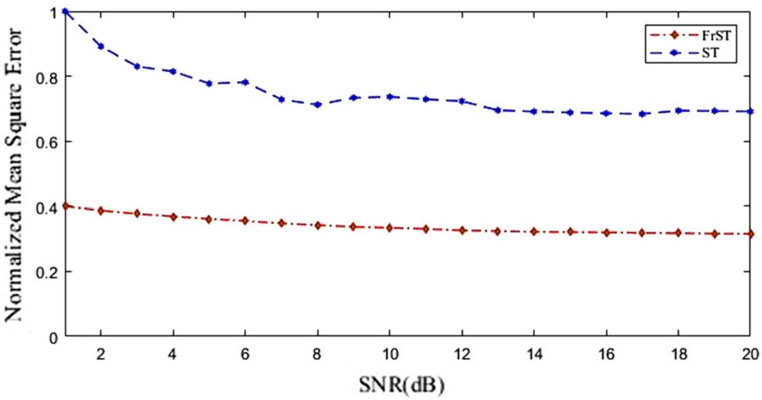

Fig. 7 Mean square error of FrST and ST

$$\int_{-\infty}^{\infty} X^{\alpha}(\tau,\ v)d\tau = X_{\alpha}(v) \tag{47}$$

So, the IFrST is define as [115]

$$x(t) = \int_{-\infty}^{\infty} X_{\alpha}(v)\kappa_{\alpha}^{*}(t, v)dv \tag{48}$$

where $X_{\alpha}(v)$ is fractional FT of function x(t).

Based on the survey, properties of fractional ST are already documented in the literature [115, 130], given in Table 4.

2.9 Application of Fractional S-Transform

A signal is defined in the concept of fractional ST based on the ideas of ST and FrFT. Here, extend ST time–frequency domain to the time-fractional frequency of FrST and also study the mathematical properties of FrST likes- linearity, scaling, inverse fractional ST and time marginal condition [115]. Generalization of the results of ST on the spaces of type W is given in [116]. The FrST on space of type S is demonstrated in [117]. It is useful for the analysis of time–frequency behaviour of test function and distributions. In [118] extends the result of ultra-distribution for the FrST given by Singh to the Bohemian spaces. Since the diverse seismic signal has distinctive ideal fractional parameters which are not helpful for multichannel seismic data analysis. Therefore utilizing FrST first decay the basic frequency after that, they analyse the minimum frequency [119]. The FrST depends on the concept of time-bandwidth product criterion and time–frequency rotation property of FrFT, and furthermore, present the standardized second-order pivotal moment calculation technique for finding the optimal order; in contrast of time-bandwidth product [120]. The theory of ideal FrST is derived from the properties of FrFT and GTBP criterion. It is a novel fractional lower order ST (FLOST) time–frequency representation technique. The FLOST time–frequency sifting algorithm depends on FLOST time–frequency representation systems [121]. The properties of FrST are described in [130]. Figure 4 shows the various applications of different transforms in different areas of Geo-informatics, Image processing, Signal processing, Bio-medical, Power system and Radar signal and Communication.

Figure 5 shows that the maximum applications of ST used in the areas of image processing and digital signal processing whereas minimum applications is used in the area of radar signals and communication system.

2.10 Detection of LFM Signal in the Presence of Echo

A LFM chirp signal is a short burst sinusoidal signal with constant amplitude and its frequency varies linearly over the pulse time. Here, a scenario of radar signal processing is considered for the detection of desired signal in the presence of echo signal. The type of both desired and echo signal is a non-stationary chirp signal. For illustration of detection of LFM signal in the presence of echo, following expression of desired signal and echo is considered,

$$x_{in} = e^{j2\pi(bt + at^2)} \tag{49}$$

where b is the centre frequency of LFM chirp signal and chirp rate 2a. The echo signal is defined as

$$n(t) = \frac{1}{10^{SNR/20}} e^{j2\pi(dt + ct^2)} \tag{50}$$

where d is the centre frequency of LFM signal in the presence of echo and chirp rate 2c. The simulated results is computed with a = 8, b = 55, c = 5 and d = 35.

The methodology adopted for the detection of LFM signal in the presence of echo is shown in Fig. 6. First the detection of LFM signal, FrST is used as the transform technique. The optimum angle of FrST is decided by the angle where FrST of the signal is maximally concentrated in transform domain. The filter transfer function is considered as uniform distribution in the transform-domain for which the transformed signal is concentrated and non-zero. Thereafter, the inverse transform is applied to determine the filtered signal in time-domain.

Subsequently, the mean square error (MSE) of filtered signal and original signal is determined and plotted with respect to signal-to-noise ratio. Similarly the detection is performed with ST. The complete plot of MSE for these transform is shown in Fig. 7 for a comparative analysis.

This plot clearly shows that detection of LFM signal using FrST is a superior technique than the ST methods.

2.11 Conclusion

The S-transform is a useful analysing tool in time–frequency localization methods with frequency dependent resolution. It is depends on moving and scalable Gaussian window function, and compensate STFT low resolution and phase information in WT. ST is a hybrid combination of the WT and STFT. This article includes the relation of several transform with FrST followed by definition and properties of ST and FrST. Subsequently, a brief survey of ST and FrST based on its application techniques between 1996 and 2019 is presented. Thereafter, a comparative analysis is performed for the filtering of chirp signal in the presence of echo signal. This analysis clearly established that FrST is superior tool than ST.

References

1. Sheng, X., Zhang, Y., Pham, D., & Lambare, G. (2005). Antileakage Fourier transform for seismic data regularization. *Geophysics, 70*(4), V87–V95.
2. Cagatay, C., Kutay, M. A., & Ozaktas, H. M. (2000). The discrete fractional Fourier transform. *IEEE Transactions on Signal Processing, 48*(5), 1329–1337.
3. Pei, S. C., & Yeh, M. H. (1998). Two dimensional discrete fractional Fourier transform. *Signal Processing, 67*(1), 99–108.
4. Aharoni, A., Vos, C. H. R., Verhoeven, H. A., Maliepaard, C. A., Kruppa, G., et al. (2002). Nontargeted metabolome analysis by use of Fourier transform ion cyclotron mass spectrometry. *OMICS: A Journal of Integrative Biology, 6*(3), 217–234.
5. Wang, S. (2007). Applications of Fourier transform to imaging analysis. *Journal of the Royal Statistical Society*, *171*, 1–11.
6. Cheddad, A., Joan, C., Kevin, C., & Paul, M. K. (2010). Digital image steganography: Survey and analysis of current methods. *Signal Processing, 90*(3), 727–752.
7. Li, W., Zhang, D., & Xu, Z. (2002). Palam identification by Fourier transform. *International Journal of Pattern Recognition and Artificial Intelligence, 16*(4), 417–432.
8. Carbonaro, M., Paola, M., Paolo, D., & Alessandro, N. (2008). Application of Fourier transform infrared spectroscopy to legume seed flour analysis. *Food Chemistry, 108*(1), 361–368.
9. Sahu, R. K., & Mordechai, S. (2005). Fourier transform infrared spectroscopy in cancer detection. *1*(5), 635–647.
10. Rohman, A., & Man, Y. B. C. (2009). Analysis of cod-liver oil adulteration using Fourier transform infrared (FTIR) spectroscopy. *Journal of the American Oil Chemists Society, 86*(12), 1149.
11. Gazi, E., Dwyer, J., Gardner, P., Siahkali, A. G., Wade, A. P., et al. (2013). Applications of Fourier transform infrared micro spectroscopy in studies of benign prostate and prostate cancer. A pilot study. *The Journal of Pathology: A Journal of the Pathological Society of Great Britain and Ireland, 201*(1), 99–108.
12. Krishna, C. M., Kegelaer, G., Adt, I., Rubin, S., Kartha, V. B., Michel, M., et al. (2006). Combined Fourier transform infrared and Raman spectroscopic approach for identification of multidrug resistance phenotype in cancer cell lines. *Biopolymers: Original Research on Biomolecules, 82*(5), 462–470.
13. Su, X., & Chen, W. (2001). Fourier transform profilometry: A review. *Optics and Lasers in Engineering, 35*(5), 263–284.
14. Vurpillot, F., Geuser, F. D., Costa, G. D., & Blavette, D. (2004). Application of Fourier transform and autocorrelation to cluster identification in the three-dimensional atom probe. *Journal of Microscopy, 216*(3), 234–240.
15. Sun, H. B., Liu, G. S., Gu, H., & Su, W. M. (2002). Application of the fractional Fourier transform to moving target detection in airborne SAR. *IEEE Transactions on Aerospace and Electronic Systems, 38*(4), 1416–1424.
16. Kutay, A., Ozaktas, H. M., Ankan, O., & Onural, L. (1997). Optimal filtering in fractional Fourier domains. *IEEE Transactions on Signal Processing, 45*(5), 1129–1143.
17. Sejdic, E., Djurovic, I., & Stankovic, L. (2011). Fractional Fourier transform as a signal processing tool: An overview of recent developments. *Signal Processing, 91*(6), 1351–1369.
18. Liu, Z., Li, S., Liu, W., Wang, Y., & Liu, S. (2013). Image encryption algorithm by using fractional Fourier transform and pixel scrambling operation based on double random phase encoding. *Optics and Lasers in Engineering, 51*(1), 8–14.
19. Jindal, N., & Singh, K. (2010). Image encryption using discrete fractional transforms. In *2010 International conference on advances in recent technologies in communication and computing* (pp. 165–167).
20. Prasad, A., Kumar, M., & Choudhury, D. R. (2012). Color image encoding using fractional Fourier transformation associated with wavelet transformation. *Optics Communications, 285*(6), 1005–1009.
21. Martone, M. (2001). A multicarrier system based on the fractional Fourier transform for time–frequency-selective channels. *IEEE Transactions on Communications, 49*(6), 1011–1020.
22. Tao, R., Li, Y. L., & Wang, Y. (2010). Short-time fractional Fourier transform and its applications. *IEEE Transactions on Signal Processing, 58*(5), 2568–2580.
23. Allen, J. B., & Rabiner, L. R. (1977). A unified approach to short-time Fourier analysis and synthesis. *Proceedings of the IEEE, 65*(11), 1558–1564.
24. Bartosch, T., & Seidl, D. (1999). Spectrogram analysis of selected tremor signals using short-time Fourier transform and continuous wavelet transform. *Annali di Geofisica, 42*(3), 497–506.

25. Hong, J. C., Sun, K. H., & Kim, Y. Y. (2005). Dispersion-based short-time Fourier transform applied to dispersive wave analysis. *The Journal of the Acoustical Society of America, 117*(5), 2949–2960.
26. Mendlovic, D., Zalevsky, Z., David, M. D., García, J., & Ferreira, C. (1997). Fractional wavelet transform. *Applied Optics, 36*(20), 4801–4806.
27. Shi, J., Xiaoping Liu, X., & Zhang, N. (2015). Multiresolution analysis and orthogonal wavelets associated with fractional wavelet transform. *Signal, Image and Video Processing, 9*(1), 211–220.
28. Chang, S. G., Yu, B., & Vetterli, M. (2000). Adaptive wavelet thresholding for image denoising and compression. *IEEE Transactions on Image Processing, 9*(9), 1532–1546.
29. Barni, M., Bartolini, F., & Piva, A. (2001). Improved wavelet-based watermarking through pixel-wise masking. *IEEE Transactions on Image Processing, 10*(5), 783–791.
30. Kabir, M. A., & Shahnaz, C. (2012). Denoising of ECG signals based on noise reduction algorithms in EMD and wavelet domains. *Biomedical Signal Processing and Control, 7*(5), 481–489.
31. Unser, M., Aldroubi, A., & Laine, A. F. (2003). Guest editorial: wavelets in medical imaging. *IEEE Transactions on Medical Imaging, 22,* 285–288.
32. Phinyomark, A., Limsakul, C., & Phukpattaranont, P. (2011). Application of wavelet analysis in EMG feature extraction for pattern classification. *Measurement Science Review, 11*(2), 45–52.
33. Ovanesova, A. V., & Suarez, L. E. (2004). Applications of wavelet transforms to damage detection in frame structures. *Engineering Structures, 26*(1), 39–49.
34. Prasad, A., & Kumar, P. (2015). Fractional wavelet transform in terms of fractional convolution. *Progress in Fractional Differentiation, 1,* 201–210.
35. Shi, J., Zhang, N. T., & Liu, X. P. (2012). A novel fractional wavelet transform and its applications. *Science China Information Sciences, 55*(6), 1270–1279.
36. Stockwell, R. G., Mansinha, L., & Lowe, R. P. (1996). Localization of the complex spectrum: the S transform. *IEEE Transactions on Signal Processing, 44*(4), 998–1001.
37. Adams, M. D., Kossentini, F., & Ward, R. K. (2002). Generalized S -transform. *IEEE Transactions on Signal Processing, 50*(11), 2831–2842.
38. Dehghani, M. J. (2009). Comparison of S-transform and wavelet transform in power quality analysis. *World Academy of Science, Engineering and Technology, 50*(4), 395–398.
39. Ranjan, R., Singh, A. K., & Jindal, N. (2018). Formulation of some useful theorems for S-transform. *Optik, 168,* 913–919.
40. Aldas, G. U. (2005). Application of the Stockwell transform to blasting-induced ground vibration. *International Journal of Surface Mining, Reclamation, and Environment, 19*(2), 100–107.
41. Sejdic, E., Stankovic, L., Dakovic, M., & Jin Jiang, J. (2008). Instantaneous frequency estimation using the S-transform. *IEEE Signal Processing Letters, 15,* 309–312.
42. Qiang, G., Molahajloo, S., & Wong, M. W. (2010). Phases of modified Stockwell transforms and instantaneous frequencies. *Journal of Mathematical Physics, 51*(5), 052101.
43. Wang, L., & Xiaofeng, M. (2011). An adaptive generalized S-transform for instantaneous frequency estimation. *Signal Processing, 91*(8), 1876–1886.
44. Ali, M., Bouguila, Z., Abdeslam, D. O., & Dieterlen, A. (2015). A new optimized Stockwell transform applied on synthetic and real non-stationary signals. *Digital Signal Processing, 46,* 226–238.
45. Hindley, N. P., Smith, N. D., Wright, C. J., Rees, D. A. S., & Mitchell, N. J. (2016). A two-dimensional Stockwell transform for gravity wave analysis of AIRS measurements. *Atmospheric Measurement Techniques, 9*(6), 2545–2565.
46. Huang, Z., Zhang, J., ZhaoZhao, T., & Sun, Y. (2016). Synchrosqueezing S-transform and its application in seismic spectral decomposition. *IEEE Transactions on Geoscience and Remote Sensing, 54*(2), 2817–2825.
47. Fei, S., Xue, X., Sun, J., Wang, J., & Zhang, Y. (2016). A SAR image despeckling method based on two-dimensional S-transform shrinkage. *IEEE Transactions on Geoscience and Remote Sensing, 54*(5), 3025–3034.
48. Ghaffarzadeh, H. (2016). A classification method for pulse-like ground motions based on S-transform. *Natural Hazards, 84*(1), 335–350.
49. Mansinha, L., Stockwell, R. G., & Lowe, R. P. (1997). Pattern analysis with two-dimensional spectral localization: Applications of two-dimensional S-transforms. *Physica A: Statistical Mechanics and its Applications, 239*(1–3), 286–295.
50. Pinnegar, C. R., & Eaton, D. W. (2003). Application of the S -transform to prestack noise attenuation filtering. *Journal of Geophysical Research: Solid Earth, 108*(B9).
51. Schimmel, M., & Gallart, J. (2005). The inverse S-transform in filters with time–frequency localization. *IEEE Transactions on Signal Processing, 53*(11), 4417–4422.
52. Stockwell, R. G. (2007). A basis for efficient representation of the S-transform. *Digital Signal Processing, 17*(1), 371–393.

53. Pei, S. C., & Wang, P. W. (2007). Modified inverse S -transform for filtering in time–frequency spectrum. In *2007 IEEE international conference on acoustics, speech and signal processing-ICASSP'07* (Vol. 3, pp. III–1169).
54. Assous, S., & Boashash, B. (2012). Evaluation of the modified S-transform for time–frequency synchrony analysis and source localization. *EURASIP Journal on Advances in Signal Processing, 2012*(1), 49.
55. Singh, S. K. (2012). The S -transform on spaces of type S. *Integral Transforms and Special Functions, 23*(7–8), 481–494.
56. Singh, S. K. (2012). The S-transform on spaces of type W. *Integral Transforms and Special Functions, 23*(12), 891–899.
57. Hutníková, M. (2013). On the range of Stockwell transforms. *Applied Mathematics and Computation, 219*(17), 8904–8909.
58. Ditommaso, R., Ponzo, F. C., & Auletta, G. (2015). Damage detection on framed structures: modal curvature evaluation using Stockwell transform under seismic excitation. *Earthquake Engineering and Engineering Vibration, 14*(2), 265–274.
59. Battisti, U., & Riba, L. (2016). Window-dependent bases for efficient representations of the Stockwell transform. *Applied and Computational Harmonic Analysis, 40*(2), 292–320.
60. Zhao, Z., Wang, S., Zhang, W., & Xie, Y. (2016). A novel automatic modulation classification method based on Stockwell-transform and energy entropy for underwater acoustic signals. In *2016 IEEE international conference on signal processing, communications and computing (ICSPCC)* (pp. 1–6).
61. Hamidia, M., & Amrouche, A. (2017). A new robust double-talk detector based on the Stockwell transform for acoustic echo cancellation. *Digital Signal Processing, 60*(2017), 99–112.
62. Yin, B., Sun, Z., Yi, Z., & He, Y. (2017). A novel local transform inverse S-transform algorithm for statistical filter. *IOP Conference Series: Materials Science and Engineering, 242*(1), 012118.
63. Bender, C. (2003). An S-transform approach to integration with respect to a fractional Brownian motion. *Bernoulli, 9*(6), 955–983.
64. Saraç, Z. (2008). Analysis of white-light interferograms by using Stockwell transform. *Optics and Lasers in Engineering, 46*(11), 823–828.
65. Weishi, M., & Jinghuai, G. (2009). Statistical denoising of signals in the S-transform domain. *Computers & Geosciences, 35*(6), 1079–1086.
66. Zidelmal, Z., Hamil, H., Moukadem, A., Amirou, A., & Abdeslam, D. Q. (2017). S-transform based on compact support kernel. *Digital Signal Processing, 62,* 137–149.
67. Sahoo, B. C., Thomas, O., Misra, D., & Newby, G. (2007). Using the one-dimensional S-transform as a discrimination tool in classification of hyperspectral images. *Canadian Journal of Remote Sensing, 33*(6), 551–560.
68. Drabycz, S. D., Stockwell, R. G., & Mitchell, J. R. (2009). Image texture characterization using the discrete orthonormal S-transform. *Journal of Digital Imaging, 22*(6), 696.
69. Mohua, J., Chen, W., Zheng, Z., & Zhong, M. (2012). Fringe pattern analysis by S-transform. *Optics Communications, 285*(3), 209–217.
70. Badrinath, G. S., & Gupta, P. (2011). Stockwell transform based palm-print recognition. *Applied Soft Computing, 11*(7), 4267–4281.
71. Zhong, M., Chen, W., Su, X., Zheng, Y., & Shen, Q. (2013). Optical 3D shape measurement profilometry based on 2D S-transform filtering method. *Optics Communications, 300,* 129–136.
72. Min, Z., Chen, W., Wang, T., & Su, X. (2013). Application of two-dimensional S -transform in fringe pattern analysis. *Optics and Lasers in Engineering, 51*(10), 1138–1142.
73. Qiuju, S., Chen, W., Zhong, M., & Su, X. (2014). An improving fringe analysis method based on the accuracy of S-transform profilometry. *Optics Communications, 322,* 8–15.
74. Dash, K. S., Puhan, N. B., & Panda, G. (2014). Non-redundant Stockwell transform based feature extraction for handwritten digit recognition. In *2014 international conference on signal processing and communications (SPCOM)* (pp. 1–4).
75. Shahla, S., & Charkari, N. M. (2014). Palm print authentication based on discrete orthonormal S -transform. *Applied Soft Computing, 21,* 341–351.
76. Kumar, M., & Agrawal, S. (2015). Color image encoding in DOST domain using DWT and SVD. *Optics & Laser Technology, 75,* 138–145.
77. Nithya, B., Sankari, Y. B., Manikantan, K., & Ramachandran, S. (2015). Discrete orthonormal Stockwell transform based feature extraction for pose-invariant face recognition. *Procedia Computer Science, 45,* 290–299.
78. Kumar, M., & Vaish, A. (2017). Encryption of color images using MSVD in DCST domain. *Optics and Lasers in Engineering, 88,* 51–59.

79. Wang, Y., & Orchard, J. (2008). Symmetric discrete orthonormal Stockwell transform. *AIP Conference Proceedings, 1048*(1), 585–588.
80. Wang, Y., & Orchard, J. (2009). Fast discrete orthonormal Stockwell transform. *SIAM Journal on Scientific Computing, 31*(5), 4000–4012.
81. Wang, Y., & Orchard, J. (2009). On the use of the Stockwell transform for image compression. In *Image processing: Algorithms and systems VII* (Vol. 7245, p. 724504). International Society for Optics and Photonics.
82. Wang, Y., & Orchard, J. (2009). The discrete orthonormal Stockwell transform for image restoration. In *2009 16th IEEE international conference on image processing (ICIP)* (pp. 2761–2764).
83. Das, M. K., & Ari, S. (2013). Analysis of ECG signal denoising method based on S-transform. *Irbm, 34*(6), 362–370.
84. Ari, S., Das, M. K., & Chacko, A. (2013). ECG signal enhancement using S-transform. *Computers in Biology and Medicine, 43*(6), 649–660.
85. Agrawal, J. P., & Vijay, R. (2013). Time–frequency filtering with the S-transform of ECG signals. *International Journal of Scientific and Research Publications, 3*(2), 1–5.
86. Zahia, Z., Amirou, A., Abdeslam, D. Q., Moukadem, A., & Dieterlen, A. (2014). QRS detection using S-transform and Shannon energy. *Computer Methods and Programs in Biomedicine, 116*(1), 1–9.
87. Hariharan, M., Vijean, V., Sindhu, R., Divakar, P., Saidatul, A., & Yaacob, S. (2014). Classification of mental tasks using Stockwell transform. *Computers & Electrical Engineering, 40*(5), 1741–1749.
88. Yusof, Y. W. M., & Saparon, A. (2015). Performance comparison of discrete orthonormal S-transform for the reconstruction of medical images. In *2015 IEEE European modelling symposium (EMS)* (pp. 128–132).
89. Raj, S., Ray, K. C., & Om Shankar, O. (2016). Cardiac arrhythmia beat classification using DOST and PSO tuned SVM. *Computer Methods and Programs in Biomedicine, 136,* 163–177.
90. Vikneswaran, V., Hariharan, M., & Mansor, M. N (2016). Analysing selected visual anomaly through ST-based multi-resolution VEP decomposition. In *2016 IEEE 12th international colloquium on signal processing & its applications (CSPA)* (pp. 64–67).
91. Raj, S., & Ray, K. C. (2017). ECG signal analysis using DCT-based DOST and PSO optimized SVM. *IEEE Transactions on Instrumentation and Measurement, 66*(3), 470–478.
92. Mario, O., Ugarte, M. R., Ianez, E., & Azorín, J. M. (2017). Application of the Stockwell transform to electroencephalographic signal analysis during gait cycle. *Frontiers in Neuroscience, 11,* 660.
93. Alan, P. V., Beltran, C. G., Sibaja, A. M., & Gómez, R. P. (2018). Use of the Stockwell transform in the detection of P300 evoked potentials with low-cost brain sensors. *Sensors, 18*(5), 1483.
94. Xianyong, X., Xu, F., & Yang, H. (2009). Short duration disturbance classifying based on S-transform maximum similarity. *International Journal of Electrical Power & Energy Systems, 31*(7), 374–378.
95. Sekhar, B. H., Dash, P. K., & Biswal, B. (2010). Power quality time series data mining using S-transform and fuzzy expert system. *Applied Soft Computing, 10*(3), 945–955.
96. Bing, L., Zhang, P. L., Liu, D. S., Mi, S. S., Ren, G. Q., & Tian, H. (2011). Feature extraction for rolling element bearing fault diagnosis utilizing generalized S transform and two-dimensional non-negative matrix factorization. *Journal of Sound and Vibration, 330*(10), 2388–2399.
97. Murat, U., Yildirim, S., & Gencoglu, M. T. (2009). An expert system based on S-transform and neural network for automatic classification of power quality disturbances. *Expert Systems with Applications, 36*(3), 5962–5975.
98. Roy, N., & Bhattacharya, K. (2013). Identification and classification of fault in an EHV transmission line using S-transform and neural network. *International Journal of Electrical, Electronics and Computer Engineering, 2*(2), 80–87.
99. Yulieth, J., Duarte, C., Petit, J., & Carrillo, G. (2014). Feature extraction for nonintrusive load monitoring based on S -transform. In *2014 Clemson university power systems conference* (pp. 1–5).
100. Borin, V. P., Barriquello, C. H., & Campos, A. (2015). Approach for home appliance recognition using vector projection length and Stockwell transform. *Electronics Letters, 51*(24), 2035–2037.
101. Singh, S. K., & Kalita, B. (2015). The S-transform on Hardy spaces and its duals. *International Journal of Analysis and Applications, 7*(2), 171–178.
102. Kunjin, C., Huang, C., & He, J. (2016). Fault detection, classification and location for transmission lines and distribution systems: A review on the methods. *High Voltage, 1*(1), 25–33.
103. Pujiantara, M., Okky Anggriawan, D., Tjahjono, A., Priyadi, A., & Hery Purnomo, M. (2017). Real-time power quality analysis for industrial power systems based on Fast S-Transform. *International Review of Electrical Engineering (IREE), 12*(3), 277. https://doi.org/10.15866/iree.v12i3.11947.
104. Reddy, M. J. B., Gopakumar, P., & Mohanta, D. K. (2016). A novel transmission line protection using DOST and SVM. *Engineering Science and Technology, an International Journal, 19*(2), 1027–1039.

105. Shuqing, Z., Li, P., Zhang, L., Li, H., Jiang, W., & Hu, Y. (2016). Modified S -transform and ELM algorithms and their applications in power quality analysis. *Neurocomputing, 185,* 231–241.
106. Mahela, O. P., & Shaik, A. G. (2017). Power quality recognition in distribution system with solar energy penetration using S-transform and fuzzy C-means clustering. *Renewable Energy, 106,* 37–51.
107. Ranjan, R., Jindal, N., & Singh, A. K. (2019). A sampling theorem with error estimation for S-transform. *Integral Transforms and Special Functions, 30,* 1–21.
108. Chang, P. S., Wang, P. W., Ding, J. J., & Wen, C. C. (2011). Elimination of the discretization side-effect in the S-transform using folded windows. *Signal Processing, 91*(6), 1466–1475.
109. Ma, J., & Li, Q. (2011). Surface wave suppression with joint S transform and TT transform. *Procedia Earth and Planetary Science, 3,* 246–252.
110. Kumar, A., Srikanth, P., & Naik, K. A. (2011). Identification of power quality events using inverse properties of S transform. In *2011 IEEE/PES power systems conference and exposition* (pp. 1–7).
111. Yanghong, T., Sun, Y., & Yin, X. (2013). Analog fault diagnosis using S-transform pre-processor and a QNN classifier. *Measurement, 46*(7), 2174–2183.
112. Pedro, S., Montoya, F. G., Agugliaro, F. M., & Gil, C. (2013). Genetic algorithm for S-transform optimisation in the analysis and classification of electrical signal perturbations. *Expert Systems with Applications, 40*(17), 6766–6777.
113. Ahmed, A., Zidelmal, Z. A., Aidene, M. & Merckle, J. (2014). Using S-transform and Shannon energy for electrical disturbances detection. In *IECON 2014-40th annual conference of the IEEE industrial electronics society* (pp. 2452–2457).
114. Kumar, R., Singh, B., Shahani, D. T., Chandra, A., & Haddad, K. A. (2015). Recognition of power-quality disturbances using S-transform-based ANN classifier and rule-based decision tree. *IEEE Transactions on Industry Applications, 51*(2), 1249–1258.
115. Ping, X. D., & Guo, K. (2012). Fractional S transform—Part 1: Theory. *Applied Geophysics, 9*(1), 73–79.
116. Singh, S. K. (2013). The fractional S-transform on spaces of type W. *Journal of Pseudo-Differential Operators and Applications, 4*(2), 251–265.
117. Singh, S. K. (2013). The fractional S-transform on spaces of type S. *Journal of Mathematics, 2013,* 1–9.
118. Singh, A. (2015). Fractional S-transform for Boehmians. *Journal of Analysis & Number Theory, 3*(2), 103–108.
119. Cong, D. Z., Xu, D. P., & Zhang, J. M. (2016). Fractional S-transform-part 2: Application to reservoir prediction and fluid identification. *Applied Geophysics, 13*(2), 343–352.
120. Wang, Y., & Zhenming, P. (2016). The optimal fractional S transform of the seismic signal based on the normalized second-order central moment. *Journal of Applied Geophysics, 129,* 8–16.
121. Junbo, L., Wang, H., Zha, D., Li, P., Xie, H., & Mao, L. (2017). Applications of fractional lower order S transform time–frequency filtering algorithm to machine fault diagnosis. *PLoS ONE, 12*(4), e0175202.
122. Sifuzzaman, M., Islam, M. R., & Ali, M. Z. (2009). Application of wavelet transform and its advantages compared to Fourier transform. *Journal of Physical Sciences, 13,* 121–134.
123. Gaunaurd, G. C., & Strifors, H. C. (2003). Applications of (Wigner-type) time–frequency distributions to sonar and radar signal analysis. arXiv preprint physics/0309050.
124. Umapathy, K., Ghoraani, B., & Krishnan, S. (2010). Audio signal processing using time–frequency approaches coding, classification, fingerprinting, and watermarking. *EURASIP Journal on Advances in Signal Processing, 2010,* 1.
125. Cohen, L. (1989). Time–frequency distributions-a review. *Proceedings of the IEEE, 77*(7), 941–981.
126. Shafi, I., Ahmad, J., Shah, S. I., Ikram, A. A., Khan, A. A., et al. (2014). High-resolution time–frequency methods performance analysis. *EURASIP Journal on Advances in Signal Processing, 2010,* 14.
127. Stanković, S. (2010). Time–frequency analysis and its application in digital watermarking. *EURASIP Journal on Advances in Signal Processing, 2010*(1), 579295.
128. Blain, G. M., Meste, O., Blain, A., & Bermon, S. (2009). Time–frequency analysis of heart rate variability reveals cardiolocomotor coupling during dynamic cycling exercise in humans. *American Journal of Physiology-Heart and Circulatory Physiology, 296,* H1651–H1659.
129. Cerutti, S. (2013). On time–frequency techniques in biomedical signal analysis. *Methods of Information in Medicine, 52*(04), 277–278.
130. Ranjan, R., Jindal, N., & Singh, A. K. (2019). Convolution theorem with its derivatives and multiresolution analysis for fractional S-transform. *Circuits, Systems, and Signal Processing, 38,* 1–24.

Rajeev Ranjan received the B.Tech. degree in Electronics and Telecommunication Engineering from Biju Patnaik University of Technology, Odisha, India, M.Tech. degree in Electronics and Communication Engineering in 2016 from Jaypee Institute of Information Technology, Noida, India and Ph.D. in Electronics and Communication Engineering from Thapar Institute of Engineering and Technology, Patiala, Punjab. Currently he is working as Assistant Professor in the Department of Electronics and Communication Engineering, Chandigarh University, Mohali, Punjab, India. His research interest in Digital Signal Processing and Communication.

Neeru Jindal received the B.Tech. and M.Tech. degree in Electronics and Communication in 2002 and 2007 respectively from Punjab Technical University, Jalandhar, Punjab, India. She has received Ph.D. degree in 2014 from the Department of Electronics and Communication Engineering, Thapar Institute of Engineering and Technology, Patiala, Punjab, India. She has been involved in various research activities in the area of image and video processing. She holds the position of Assistant Professor in the Department of Electronics and Communication Engineering, Thapar Institute of Engineering and Technology Patiala, Punjab, India.

A. K. Singh has completed his B.Tech. in I & E Engineering in year July 2001 from M.I.E.T., Meerut. He joined M.I.T.S., Gwalior as M.Tech student in Microwave Engineering in year 2003 and completed his M.Tech. in 2005. He did his Ph.D. from Department of Electronics and Communication Engineering, Jaypee University of Engineering & Technology, Guna in year 2011 with the specialization in digital signal processing. Currently he is working as Associate Professor in the Department of Electronics and Communication, Thapar University Patiala, (Punjab) India. His research interest in speech signal processing, Digital Signal Processing and communication.